ISBN: 978-3-95450-234-9 ISSN: 2673-5504 doi:10.18429/JACoW-SRF2023-WEPWB101

PRESENT STATUS OF RIKEN POWER COUPLERS FOR SRILAC

K. Ozeki†, O. Kamigaito, N. Sakamoto, K. Suda, K. Yamada
RIKEN Nishina Center, Wako, Japan

Abstract

The heavy ion linac of the RIKEN, utilizing superconducting technology, began operations in September 2019. Over the following 13 months, two of the ten superconducting accelerating cavities experienced vacuum leaks from the vacuum windows of the fundamental power couplers (FPCs). Currently, additional vacuum windows are installed on all ten FPCs, and the beam supply continues without encountering any major issues with the FPCs. Additionally, the fabrication of ten replacement FPCs has been completed, addressing the underlying issues that led to the deterioration of the vacuum window strength. Currently, we are conducting radio frequency (RF) process of the new FPCs. In addition, we are designing a bias applying component to suppress multipacting in the FPCs. This paper reports the status of these issues related to the FPCs at the RIKEN.

INTRODUCTION

In RIKEN Nishina Center, the RIKEN Heavy Ion Linac (RILAC) [1] had been used to supply intense beams for the synthesis of super-heavy elements (SHEs) [2]. Additionally, it serves as an injector for the following radio isotope beam factory (RIBF) accelerator complex comprising four ring cyclotrons [3].

RILAC has been upgraded for the synthesis of new SHEs ($Z > 118$) and production of radioactive isotopes for medical use. As part of this upgrade, a superconducting linac (SRILAC) [4-10] was constructed and installed downstream of the RILAC (see Fig. 1) to enhance the acceleration voltage. The SRILAC consists of three cryomodules with ten superconducting quarter-wavelength resonators (SC-QWRs). The two upstream cryomodules have four SC-QWRs each, and the one downstream cryomodule has two SC-QWRs.

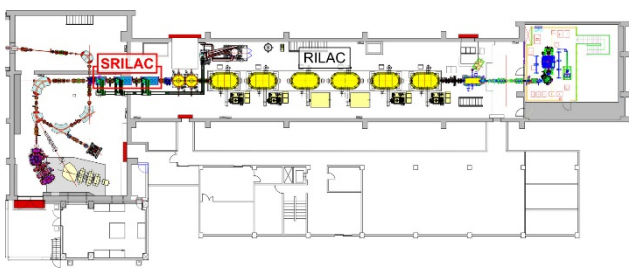

Figure 1: Overview of the RILAC and SRILAC.

Each SC-QWR was equipped with a fundamental power coupler (FPC) with a single-disc-type vacuum window. A schematic representation of the FPC is shown in Fig. 2. The inner conductor (IC) and outer conductor (OC) are composed of bulk copper and copper-plated stainless steel, respectively. A thermal anchor was connected to a thermal shield cooled using liquid nitrogen.

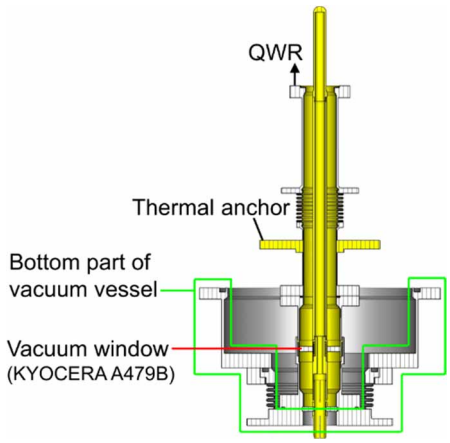

Figure 2: Schematic of the FPC.

VACUUM LEAKS FROM FPCS

The installation of cryomodules on the beamline was completed in March 2019, and the cooling tests began in September 2019. In November, during repeated cooling tests, the first vacuum leak occurred in the vacuum window of an FPC. The vacuum leakage into the cavity was stopped via an evacuation from the atmospheric side of the vacuum window (the RF supply to that cavity was no longer available). Beam acceleration tests were conducted using the remaining nine SC-QWRs, and the beam supply for the new SHE synthesis experiments began in June 2020.

The second vacuum leak occurred at another FPC in October 2020. The condition of the atmospheric side of the vacuum window was examined for all FPCs, and the dew condensation and rust were observed. The metallization of alumina used for the vacuum window deteriorated owing to galvanic corrosion, and the strength of the vacuum window brazing was reduced. This deterioration may have led to the vacuum leak. The vacuum leakage was stopped using the same method employed during the initial incident. The beam supply was continued using the remaining eight SC-QWRs, while dry nitrogen was introduced around the vacuum windows of the remaining eight FPCs to prevent dew condensation. Simultaneously, additional vacuum windows (outer windows) were developed, described in the next section.

INSTALLATION OF OUTER WINDOWS

To enable radio frequency (RF) supply and restore the two SC-QWRs that were no longer available for beam acceleration, outer windows were developed. A schematic of

† k_ozeki@riken.jp

ISBN: 978-3-95450-234-9 ISSN: 2673-5504 doi:10.18429/JACoW-SRF2023-WEPWB101

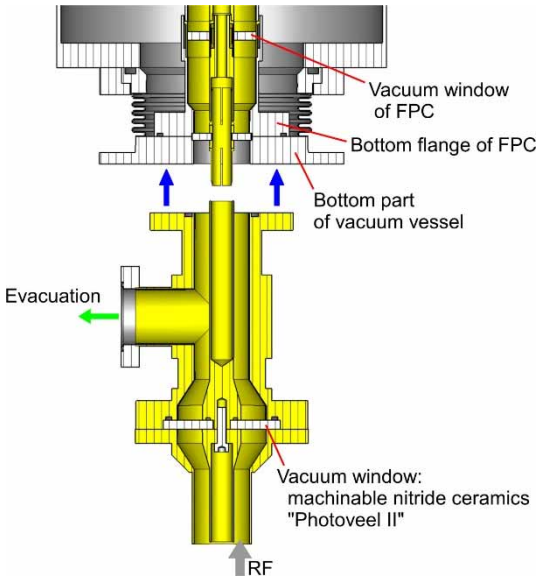

Figure 3: Schematic of the outer window.

the outer window is shown in Fig. 3. These windows utilized a machinable nitride ceramics called “Photoveel II” and were vacuum sealed with O-rings. Two outer windows facing each other were connected to perform vacuum sealing tests and RF tests up to 4 kW. After the successful completion of the tests, outer windows were installed on the

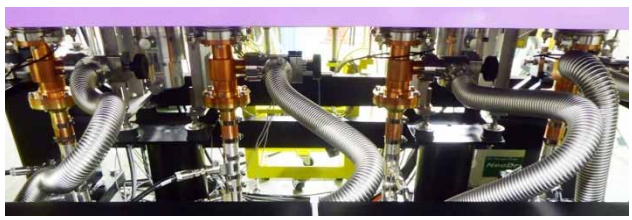

Figure 4: Photo of the outer windows installed on the FPCs.

two FPCs with vacuum leaks. Consequently, beam supply using all ten SC-QWRs was achieved.

Because the usability of the outer windows was confirmed, additional units were fabricated and installed on all remaining FPCs (Fig. 4). Since their installation, no significant issues attributable to FPCs have been reported.

NEW FPCS

After dew condensation was observed around the vacuum window, the temperature distribution in the lower part of the FPC was estimated (until then, it was assumed that the temperature around the vacuum window was not significantly different from the room temperature). As boundary conditions, the temperatures at the lowest parts of the FPC and thermal anchor were set to 300 and 80 K, respectively. The results of this estimation are shown in Fig. 5A. The low thermal conductivity of the lower part of the OC resulted in a considerable temperature difference between the bottom of the FPC and vacuum window.

The strength of the vacuum window might have been reduced even for FPCs that do not experience vacuum leaks. Therefore, we decided to fabricate and replace them with

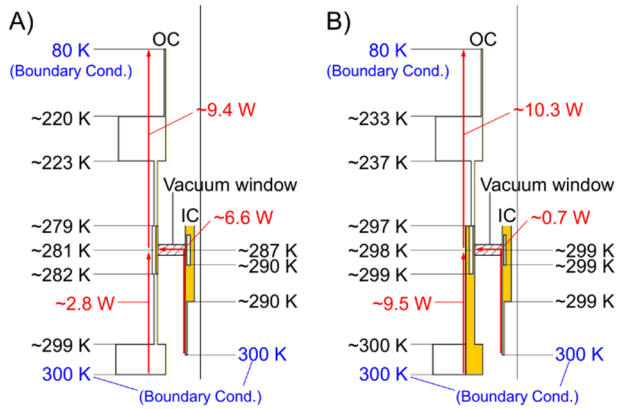

Figure 5: Temperature distribution estimations of A) present FPC and B) new FPC.

new FPCs. For the fabrication of the new FPCs, the structure was reviewed to improve the thermal conductivity of the lower part of the OC. As mentioned previously, the OC of the present FPC was made of copper-plated stainless steel. In the new FPC, the OC was made of thicker copper. The estimated temperature distribution of the new FPC is shown in Fig. 5B. The temperature around the vacuum window is expected to be approximately equal to the temperature at the bottom of the FPC. To ensure safety, a ribbon heater will be also installed around the vacuum window.

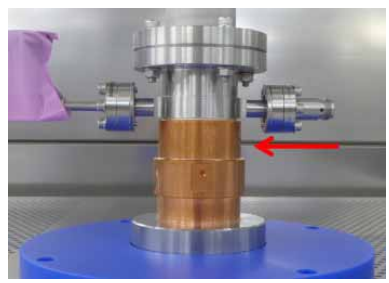

Figure 6: Photo of lower part of new FPC. The OC from bottom flange to the vacuum window (the position is indicated by a red arrow) is made of thin copper.

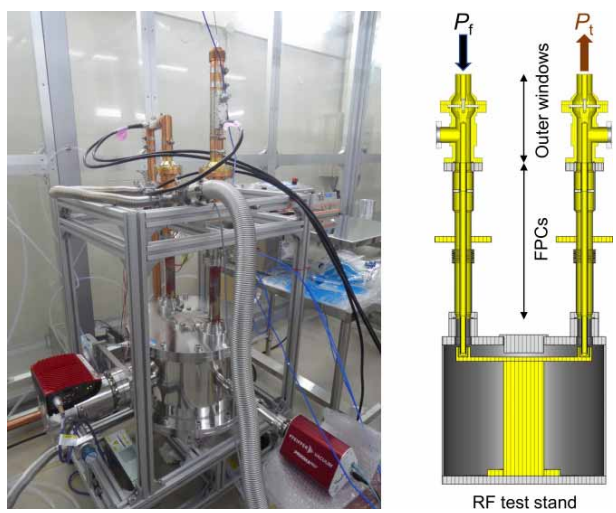

Figure 7: Photo and schematic of the RF process.

ISBN: 978-3-95450-234-9 ISSN: 2673-5504 doi:10.18429/JACoW-SRF2023-WEPWB101

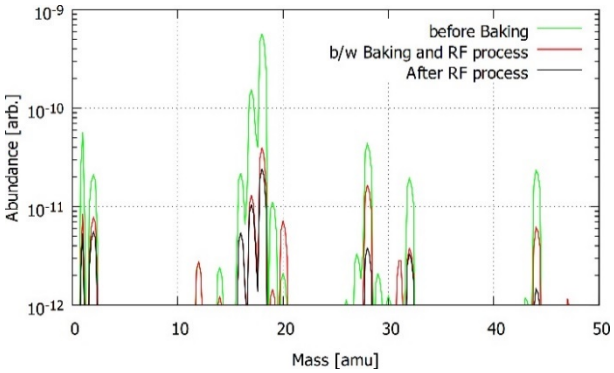

Figure 8: Transition of mass distribution of residual gas.

Ten new FPCs were delivered by November 2022 (Fig. 6). Pre-processing is currently underway in preparation for the replacement of the FPCs. All ten FPCs were cleaned in an ISO class-1 clean room. Although a brief contact with water will not adversely affect the brazing of the vacuum window, the use of ultrapure water was avoided during cleaning. Only air was used to remove the dust. The FPCs were then mounted in pairs on an RF test stand for baking and RF processing. A photograph and schematic of the RF process are shown in Fig. 7. During the RF process, the FPCs were supplied with pulsed and continuous RF up to 5 kW in traveling wave and total reflection configurations, respectively. The actual replacement of the FPCs is expected to be conducted after the successful completion of the new SHE synthesis experiment, which is currently underway. After completing the RF process, the FPCs were filled and sealed with dry nitrogen for long-term storage.

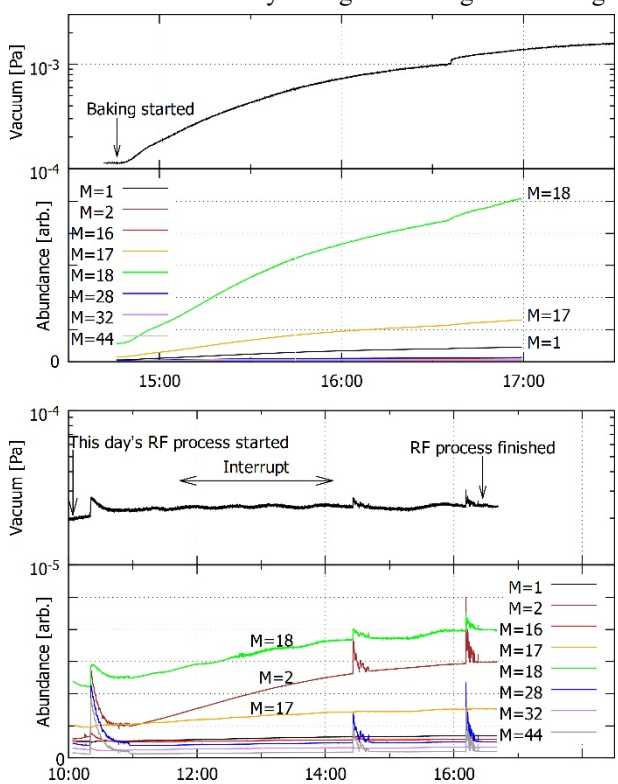

Figure 9: Variations of vacuum and abundance of outgassing with respect to time, during baking (top) and RF process (bottom).

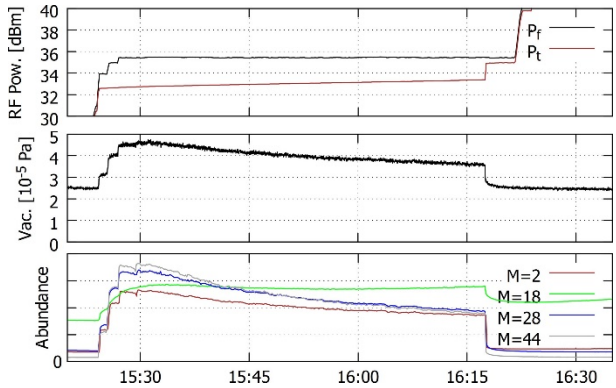

Figure 10: Variations of RF powers, vacuum, and outgassing with respect to time, during RF process.

Presently, the baking and RF processes are being performed sequentially.

During the baking and RF processes, a residual gas analyzer was installed on the RF test stand to examine the outgassing components. Examples of the mass distribution of the residual gas before baking, after baking (before the RF process), and after the RF process are shown in Fig. 8.

The time-dependent variations in the vacuum levels and abundance of outgassing during the baking and RF processes are shown in Fig. 9. Water (M = 18) was the main outgassing component during baking. During the RF process, there were significant variations in abundance for M = 2, 18, 28, and 44, corresponding to multipacting. The RF process was interrupted from approximately 11:30 to 14:00, during which the abundances of M = 2 and M = 18 continued to increase.

Figure 10 illustrates another example of multipacting. The RF powers are also shown (see Fig. 7 for P_f and P_t). When multipacting was completed, P_t increased in a staircase pattern, whereas vacuum and outgassing decreased sharply.

DEVICE FOR APPLYING BIAS TO IC

To prevent the multipacting of the FPC during operation, the fabrication of a component called bias-tee, which applies a bias voltage to the IC is currently under consideration. The maximum applied voltage is assumed to be approximately 1 kV. A schematic of the bias-tee currently under design is shown in Fig. 11. The IC on the port 1 side has a male-female tapered structure. A polyimide film is placed between them and tightened using insulating bolt to allow them to adhere to each other. A bias voltage is applied from port 3 to the IC at port 2. To prevent the leakage

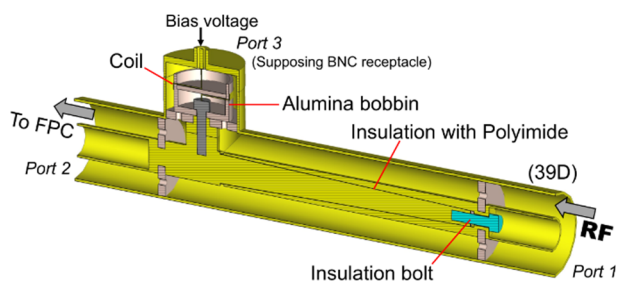

Figure 11: Schematic of a bias-tee.

ISBN: 978-3-95450-234-9 ISSN: 2673-5504 doi:10.18429/JACoW-SRF2023-WEPWB101

of the RF to the port 3 side, the conductor for the applying bias has a coiled structure. The optimum structure of the coil required to suppress the RF reflection and leakage was determined using the CST Studio Suite [11]. The detailed structure is under design in cooperation with the manufacturer.

SUMMARY

SRILAC began operations at RIKEN in 2019. Within the next 13 months, vacuum leaks occurred in two FPCs. Beam acceleration using all ten SC-QWRs is being performed by installing outer windows on the FPCs where the vacuum leaks occurred. Outer windows were installed on the other FPCs to protect the vacuum windows. Since their installation, the FPC have not encountered any serious issues.

New FPCs were fabricated for replacement, which improved the cause of vacuum leak. Actual replacement will be performed after the completion of the ongoing experiment. The pre-processing of new FPCs is currently underway. Analyse of the outgassing during the baking and RF processes were also performed.

The trial production of a component to apply a bias voltage to the IC of the FPC is being planned.

REFERENCE

[1] M. Odera *et al.*, "Variable frequency heavy-ion linac, RILAC", *Nucl. Instrum. Methods Phys. Res., Sect. A*, vol. 227, 1984. doi:10.1016/0168-9002(84)90121-9

[2] P. J. Karol, R. C. Barber, B. M. Sherrill, E. Vardaci, and T. Yamazaki, "Discovery of the elements with atomic numbers Z = 113, 115 and 117 (IUPAC Technical Report)", *Pure Appl. Chem.*, vol. 88, pp. 139-153, Feb. 2016. doi:10.1515/pac-2015-0502

[3] Y. Yano, "The RIKEN RI beam factory project: A status report", *Nucl. Instrum, Methods Phys. Res., Sect. B*, vol. 261, 2007. doi:10.1016/j.nimb.2007.04.174

[4] K. Suda *et al.*, "Fabrication and performance of superconducting quarter-wavelength resonators for SRILAC", in *Proc. SRF'19*, Dresden, Germany, Jun.-Jul. 2019, pp. 182-187. doi:10.18429/JACoW-SRF2019-MOP055

[5] K. Yamada *et al.*, "Construction of superconducting linac booster for heavy-ion linac at RIKEN Nishina Center", in *Proc. SRF'19*, Dresden, Germany, Jun.-Jul. 2019, pp. 502-507. doi:10.18429/JACoW-SRF2019-TUP037

[6] K. Yamada *et al.*, "Successful beam commissioning of heavy-ion superconducting linac at RIKEN", in *Proc. SRF'21*, East Lansing, MI, USA, Jun.-Jul. 2021, pp. 167-174. doi:10.18429/JACoW-SRF2021-MOOFAV01

[7] N. Sakamoto *et al.*, "Operation experience of the superconducting linac at RIKEN RIBF", in *Proc. SRF'21*, East Lansing, MI, USA, Jun-Jul. 2021, pp. 315-318. doi:10.18429/JACoW-SRF2021-MOPFAV005

[8] K. Yamada *et al.*, "Operational experience for RIKEN superconducting linear accelerator", presented at SRF'23, Grand Rapids, MI, USA, Jun. 2023, paper MOIXA04, this conference.

[9] T. Nishi *et al.*, "Development of non-destructive beam envelope measurements in SRILAC with low beta heavy ion beams using BPMs", presented at SRF'23, Grand Rapids, MI, USA, Jun. 2023, paper MOPMB086, this conference.

[10] N. Sakamoto *et al.*, "Degradation and recovery of cavity performance in SRILAC cryomodules at RIBF", presented at SRF'23, Grand Rapids, MI, USA, Jun. 2023, paper WEPWB085, this conference.

[11] https://www.3ds.com/products-services/simulia/products/cst-studio-suite/.